Antitumor Activity of 3-Indolylmethanamines 31B and PS121912

MARGARET L. GUTHRIE[2,3], PREETPAL S. SIDHU[2,3], EMILY K. HILL[1], TIMOTHY C. HORAN[1],
PREMCHENDAR NANDHIKONDA[2,3], KELLY A. TESKE[2,3], NINA Y. YUAN[2,3], MARINA SIDORKO[2,3],
REVATHI RODALI[2,3,] JAMES M. COOK[2,3], LANLAN HAN[2,3], NICHOLAS R. SILVAGGI[2,3],
DANIEL D. BIKLE[4], RICHARD G. MOORE[1], RAKESH K. SINGH[1] and LEGGY A. ARNOLD[2,3]

[1]*Molecular Therapeutics Laboratory, Program in Women's Oncology,*
Women and Infants' Hospital of Rhode Island, Alpert Medical School, Brown University, Providence, RI, U.S.A.;
[2]*Department of Chemistry and Biochemistry and the* [3]*Milwaukee Institute of Drug Discovery,*
University of Wisconsin, Milwaukee, WI, U.S.A.;
[4]*Endocrine Research Unit, Department of Medicine, Veterans Affairs Medical Center, San Francisco, CA, U.S.A.*

Abstract. *Aim: To investigate the in vivo effects of 3-indolylmethanamines 31B and PS121912 in treating ovarian cancer and leukemia, respectively. Materials and Methods: Terminal deoxynucleotidyl transferase dUTP nick-end labeling (TUNEL) and western blotting were applied to demonstrate the induction of apoptosis. Xenografted mice were investigated to show the antitumor effects of 3-indolylmethanamines.* [13]*C-Nuclear magnetic resource (NMR) and western blotting were used to demonstrate inhibition of glucose metabolism. Results: 31B inhibited ovarian cancer cell proliferation and activated caspase-3, cleaved poly (ADP-ribose) polymerase 1 (PARP1), and phosphorylated mitogen-activated protein kinases (MAPK), JUN N-terminal kinase/stress-activated protein kinase (JNK/SAPK) and p38. 31B reduced ovarian cancer xenograft tumor growth and PS121912 inhibited the growth of HL-60-derived xenografts without any sign of toxicity. Compound 31B inhibited de novo glycolysis and lipogenesis mediated by the reduction of fatty acid synthase and lactate dehydrogenase-A expression. Conclusion: 3-Indolylmethanamines represent a new class of antitumor agents. We have shown for the first time the in vivo anticancer effects of 3-indolylmethanamines 31B and PS121912.*

The most simple and best known member of the 3-indolylmethanamine family is gramine, a compound made by many plants for defense due to its toxicity to animals

Correspondence to: Leggy A. Arnold, University of Wisconsin Milwaukee, 3210 N. Cramer Street, Milwaukee, WI 53211-3029, U.S.A. Tel: +1 4142292612, Fax: +1 4142293029, e-mail: arnold2@uwm.edu

Key Words: 3-Indolylmethanamine, ovarian cancer, leukemia.

[lethal dose 50% $(LD_{50})\approx50$ mg/kg in rodents] (1). In the laboratory, gramine is an important precursor for tryptophan, especially when converted to the quaternary ammonium salt (Figure 1A) (2). Importantly, thiols can react with the free gramine base $(pK_b=3.4)$ at elevated temperature due to acidity of the thiol $(pK_a=10.5)$ and the basicity of the amine. Thus, the amine is converted into a quaternary ammonium group making it a good leaving group and the sulfur anion a superior nucleophile (Figure 1B) (3).

In water, protonation of gramine is accelerated under acidic conditions inducing a self-condensation reaction leading to the formation of an insoluble polymer (4). In contrast, *N*-phenyl-substituted 3-indolylmethanamines are significantly more stable in water due to a higher nitrogen pK_b value inducing selectivity towards protein targets. For instance, the 3-indolylmethanamine CCT036477 (Figure 1C) was identified as a selective inhibitor of wingless-type MMTV integration site family (WNT)-dependent transcription (5). Evan *et al*. reported that CCT036477 reduced the transcriptional activity of the T-cell factor/lymphoid enhancer factor transcription factor family at the β-catenin level. The compound was stable for 24 h at pH 7 and pH 9 but decomposed at pH 4 within that time frame. In the presence of nucleophile glutathione at pH 7, CCT036477 formed the corresponding sulfide, which was detectable after one hour by liquid chromatography–mass spectrometry/mass spectrometry (LCMS/MS). Independently, we used high-throughput screening (HTS) to identify the class of 3-indolylmethanamines as novel irreversible inhibitors of the interaction between the vitamin D receptor (VDR) and the co-regulator steroid receptor coactivator-2 using high-throughput screening (6). The initial hit compounds, similar to CCT036477, were pyridyl-substituted 3-indolylmethanamines. Structural analogs of the class of compounds bearing electron-donating groups in the *para* position alkylated VDR more
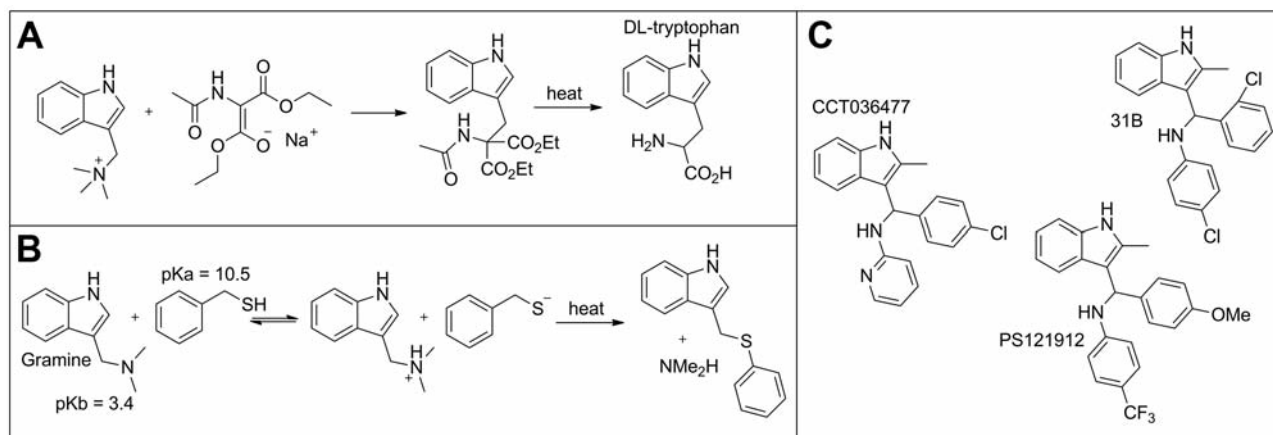
Figure 1. *Mode of action of 3-indolylmethanamines. A: Synthesis of tryptophan based on nucleophilic substitution. B: Reaction of gramine with sulfur nucleophile. C: Developed 3-indolylmethanamines.*

readily than those with electron-withdrawing groups following a correlation with decreasing pK_b values of the nitrogen. An additional strong free linear relationship using Hammett σ-values for different substituents confirmed the correlation between reaction rate and pK_b, as well as stabilization of the electrophilic transition state due to electron-donating phenyl substituents in conjugation with the protonated indole nitrogen. The selectivity of the 3-indolylmethanamine PS121912 for VDR over other nuclear receptors is remarkable (7). Like Ewan *et al.*, we observed selective transcriptional inhibition of particular genes in the presence of these compounds (8). In addition, both groups observed the induction of anti-proliferation in cancer cells mediated by the activation of caspases 3 and 7 (5, 8). Importantly, cytotoxic effects were predominantly observed in cancer cells, as well as certain types of cancer cell lines. Herein, we report the *in vivo* effects of 3-indolylmethanamines using xenografted mice to evaluate their anti-tumor activity. In addition, we demonstrated the effects of these compounds for anti-proliferative pathways in cells.

Materials and Methods

Synthesis and cell culture. 31B and PS121912 were synthesized as described earlier (6, 9). SKOV3, OVCAR8, ECC1, and HL-60 cells for these studies were obtained from the American Type Culture Collection (Manassas, VA, USA) and authenticated by short tandem repeat analysis. Cell lines were maintained in Dulbecco's modified eagle's medium (DMEM) (Gibco, Grand Island, NY, USA) or RPMI-1640 (Gibco) supplemented with 10% fetal bovine serum (Gibco) and 1% penicillin/streptomycin (Gibco). Cell cultures between 5-10 passages were maintained in 75 cm^2 flasks (Corning, New York, NY, USA) and incubated in a humidified atmosphere with 5% CO_2 at 37°C.

Cell viability assay. SKOV3, OVCAR8 and ECC1 cells (5×10^3/well) were seeded in 96-well plates (Corning) and allowed to adhere overnight before treatment with compounds or vehicle

(DMSO). After incubation at 37°C for 18 h, cell viability was determined by the Aqueous-One-Solution Assay (Promega, Madison, WI, USA). Significance values were calculated with Student's *t*-test using GraphPad Prism (La Jolla, CA, USA).

Terminal deoxynucleotidyl transferase dUTP nick-end labeling (TUNEL) assay. 31B-induced DNA nick damage was analyzed using the Roche *in situ* Cell Death Detection Kit (Branford, CT, USA). SKOV3 and OVCAR8 cells (10,000/well) were seeded in 8-well chamber slides, allowed to adhere overnight, and treated with DMSO vehicle or 15 μM 31B for 24 h in serum-supplemented DMEM. Cells were then fixed with 10% neutral buffered formalin, and stained according to the manufacturer's protocol. Slides were then cover-slipped with 4',6-diamidino-2-phenylindole (DAPI)-containing mounting medium (Vector Labs, Burlingame, CA, USA).

Western blotting. Lysates were collected, quantified for protein concentration, and separated by polyacrylamide gel electrophoresis followed by immunoblotting. Primary antibodies to cleaved poly (ADP-ribose) polymerase 1 (PARP1), cleaved caspase-3, p-p38, p-jun N-terminal kinase/stress-activated protein kinase (p-JNK/SAPK) (Cell Signaling Technology, Beverly, MA, USA), fatty acid synthase (FASN), lactate dehydrogenase A (LDHA), glyceraldehyde 3-phosphate dehydrogenase (GAPDH) (Santa Cruz Biotechnology, Santa Cruz, CA, USA) were diluted 1:1,000 in phosphate-buffered saline (PBS)-T/5% bovine serum albumin (BSA). Bands were visualized using horseradish peroxidase-conjugated secondary antibodies (Cell Signaling Technology, Danvers, MA, USA), followed by enhanced chemiluminescence (GE Healthcare, Pittsburgh, PA, USA) and documented by autoradiography (F-Bx810 Film; Phenix, Hayward, CA, USA).

Xenograft animal models. The American Association for Laboratory Animal Science protocol 13-14#04 protocol for this study was approved by University of Wisconsin Milwaukee. Female *NU/NU* mice were purchased (Charles River, Wilmington, MA, USA) at an age of 35-42 days and housed in groups of three. Animals were assigned to a treatment (n=11) or a control group (n=10). A total of 5×10^6 cells suspended in 0.1 ml Matrigel were inoculated

subcutaneously in the right flank of each animal under anesthesia (isoflurane). After seven days, vehicle (5% DMSO, 47.5% PBS, 47.5% polyethylene glycol 400 (PEG400), 31B (5 mg/kg), or PS121912 (1 mg/kg) was administered *i.p.* five days a week. Animals were weighed every week and tumor volume was determined by caliper once a week. On the last day of the study, mice were euthanized, tumors were extracted and weighed and processed for paraffin embedding followed by fluorescent immunohistochemistry. Briefly, tumor tissue was treated with primary antibody against FASN (Santa Cruz Biotechnology) and Dylight 595 secondary antibody, cover-slipped with DAPI-containing mounting medium, and imaged by confocal fluorescence microscopy.

Nuclear magnet resonance (NMR) analysis of glycolytic metabolites. ^{13}C-NMR was conducted using a 600 MHz instrument (Bruker, Billerica, MA, USA). 1.5 million SKOV3 or OVCAR8 cells were seeded onto 100-mm dishes (Corning) and allowed to adhere overnight in 5 ml of serum-supplemented DMEM. The medium was then replaced with serum and glucose-free medium containing 60 μl of 100 mM ^{13}C-labeled [1,6] glucose (Sigma Aldrich, Milwaukee, WI, USA). Cells were treated with vehicle or 15 μM 31B in 5 ml media and incubated overnight. Five hundred milliliters of medium was then collected and added into the NMR tube together with 100 μl D_2O as solvent and 5 μl DMSO as reference (~40 ppm). ^{13}C-NMR was performed with a standard inverse-gated-decoupling sequence. The area under the peak for DMSO was set as 1.0 followed by the integration of metabolite peaks pyruvate (~60 ppm), lactate (~20 ppm), and long-chain fatty acids (~30 ppm). Each experiment was performed in triplicate.

Results

The 3-indolylmethanamine 31B significantly reduced cell viability of cisplatin-resistant SKOV3 and OVCAR8 ovarian cancer cells, and ECC1 endometrial cancer cells after 18 hours at a concentration of 25 μM (Figure 2A).

At a concentration of 50 μM 31B, none of the gynecological cancer cells were viable. In addition, DNA fragmentation, visualized by TUNEL, was observed for SKOV3 and OVCAR8 cells treated at a concentration of 15 μM 31B (Figure 2B). The apoptotic cellular response was demonstrated by western blotting for the induced cleavage and activation of caspase-3 for SKOV3 and OVCAR8 and the production of cleaved PARP1 (Figure 2C) (10). In addition, we observed phosphorylation of stress-activated protein kinases SAPK/JNK and p38 for cells treated with 25 μM 31B for 18 h.

The anti-tumor efficacy of 31B and PS12192 was subsequently evaluated in SKOV3- and HL-60-derived xenograft mouse models, respectively (Figure 3).

Xenografted SKOV3 cells exhibited slow growth during the first three weeks. Treatment with 31B (5 mg/kg *i.p.*, five times/week) was started after week one. Three weeks into the study, a significant difference in tumor volume was observed between vehicle- and 31B-treated animals (Figure 3A). The difference was confirmed by the average tumor weight at day 42 (Figure 3C). During the study, normal weight gain was observed for both vehicle- and drug-treated
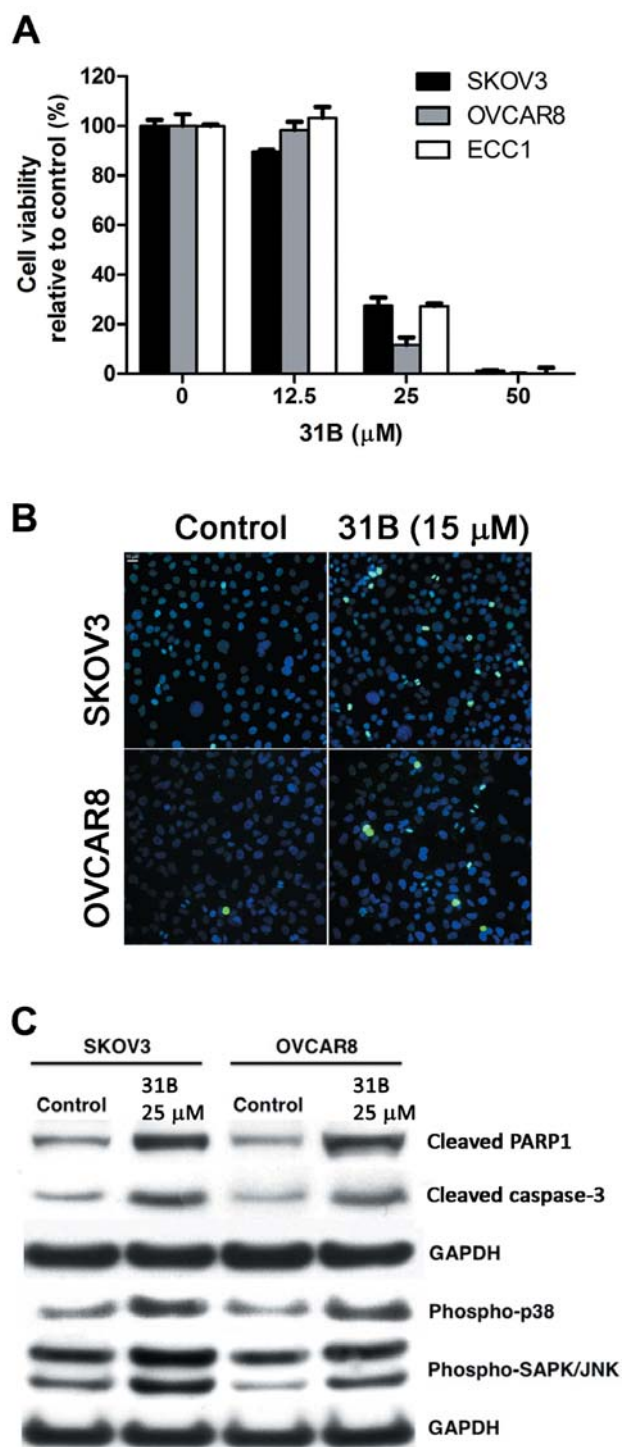
Figure 2. *Anti-proliferative effects of 31B on a panel of gynecological cancer cells. A: Cell viability of ovarian cancer cells after 18 h Data are the mean±SEM. B: Analysis of DNA fragmentation via terminal deoxynucleotidyl transferase dUTP nick end labeling (TUNEL) assay. C: Expression of apoptosis markers by western blot. GAPDH: Glyceraldehyde 3-phosphate dehydrogenase; PARP1: poly (ADP-ribose) polymerase 1; SAPK/JNK: JUN N-terminal kinase/stress-activated protein kinase.*
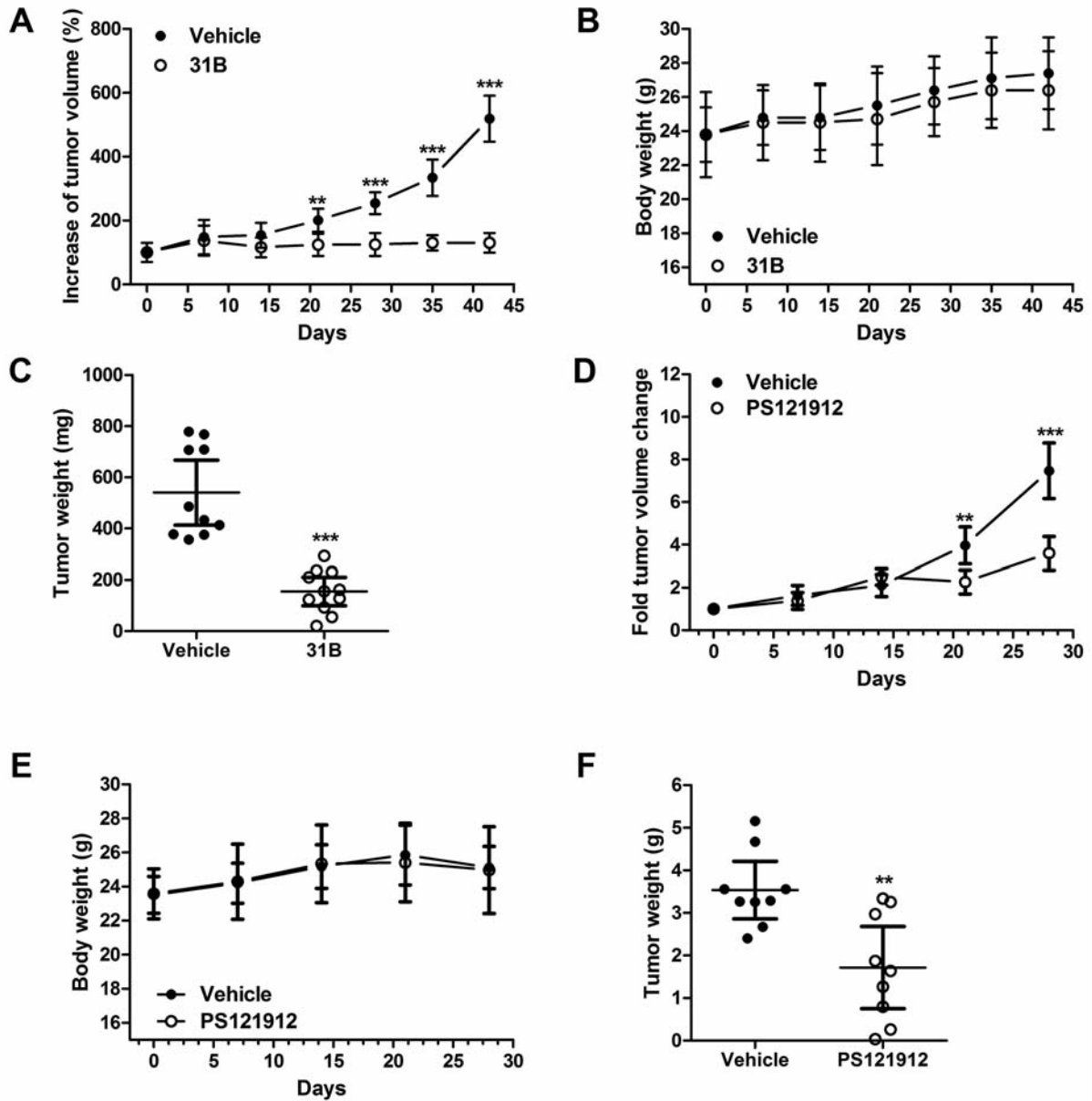
Figure 3. *Anti-tumor activity of 31B in a SKOV3-derived and PS121912 in a HL60-derived mouse xenograft model. Tumor volume, animal weight, and final tumor weight of SKOV3-derived tumor xenografts treated i.p. with 31B at 5 mg/kg five times a week (A-C, respectively) and of HL-60-derived tumor xenografts treated i.p. with PS121912 at 1 mg/kg five times a week (D-F, respectively). Data are the mean±SEM. **p< 0.001,***p<0.0001.*

mice (Figure 3B). HL-60-xenografted mice were used to demonstrate the antitumor effect of PS121912 based on earlier reported anticancer effects (8). Untreated tumors grew quickly, doubling in size each week, in contrast to PS121912-treated tumors (1 mg/kg *i.p.*, five times/week) that were significantly smaller three weeks into the study (Figure 3D). Due to the rapid growth, tumors were harvested after 28 days and exhibited significant weight differences between vehicle and PS121912-treated animals (Figure 3F). No

change in body weight was observed in treated mice in comparison to control animals (Figure 3E). The tumor tissue of 31B-treated animals was further investigated with respect to FASN expression using immunohistochemistry (results not shown). A decrease of cytoplasmic and nuclear FASN staining compared to control tissues indicated an anti-lipogenic role of 31B *in vivo*. Further *de novo* glycolysis and lipogenesis studies were carried-out with SKOV3 and OVCAR8 cells using ^{13}C-NMR and western blot.

Treatment with 15 μM 31B under normoxic conditions in SKOV3 cells significantly reduced glycolytic production of pyruvate from glucose, and pyruvate conversion to lactate (Figure 4A). Intriguingly, 31B still exhibited antiglycolytic effects under hypoxic conditions in SKOV3, where pyruvate production was reduced and lactate production significantly decreased. Although pyruvate was not detectable with OVCAR8 cells, production of lactate was significantly diminished under normoxic conditions (Figure 4B). In addition, we detected long-chain fatty acids with OVCAR8 cells as a marker of *de novo* lipid metabolites synthesized from the ^{13}C-labeled glucose. 31B significantly reduced fatty acid levels in both normoxic and hypoxic environments. These findings were supported by western blotting in SKOV3 and OVCAR8 cells, which showed that 31B treatment reduced the expression of both FASN and LDHA, which catalyzes the conversion of pyruvate to lactate (Figure 4C).

Discussion

Following literature indications that 3-indolylmethanamines possess anticancer properties, we herein demonstrated the anti-tumor effects of two VDR-co-regulator inhibitors 31B and PS121912. It has been shown that CCT036477, an analog of the two compounds characterized in this study, inhibited the growth of HT29, SW480, and HCT116 colonic cancer cells and SNU475 hepatocellular cancer cells (5). In addition, CCT036477, as an inhibitor of the WNT signaling pathway, inhibited the growth of osteosarcoma cells (Saos2) (11). This investigation of 31B in respect to cancer was prompted by the results of a screening of 60 different cancer cell lines conducted by the National Cancer Institute that demonstrated the growth reduction of 31B-treated cisplatin-resistant ovarian cancer cells SKOV3 (12). Herein, we demonstrated that the anti-proliferative effect of 31B is mediated by apoptosis in SKOV3, OVCAR8, and ECC1 cells. Importantly, this effect was recapitulated *in vivo* using xenografted mice. The *in vivo* efficacy of 3-indolylmethanamines has been known for centuries as plant toxins, but *in vivo* evaluations at sub-toxic levels with respect to cancer have been shown here for the first time. Animals exposed to these lower concentrations did exhibit normal growth, however, tumor formation was significantly reduced. Similarly, Peiffer *et al*. showed that cells from patients with chronic lymphocytic leukemia were more sensitive to CCT036477 than were healthy peripheral blood mononuclear cells emphasizing the sensitivity of cancer cells toward 3-indolylmethanamines (9). We also demonstrated *in vivo* that a dosage of 1 mg/kg PS121912 was sufficient to significantly reduce the size of tumors derived from promyelocytic leukemia cells after three weeks of treatment despite aggressive growth.

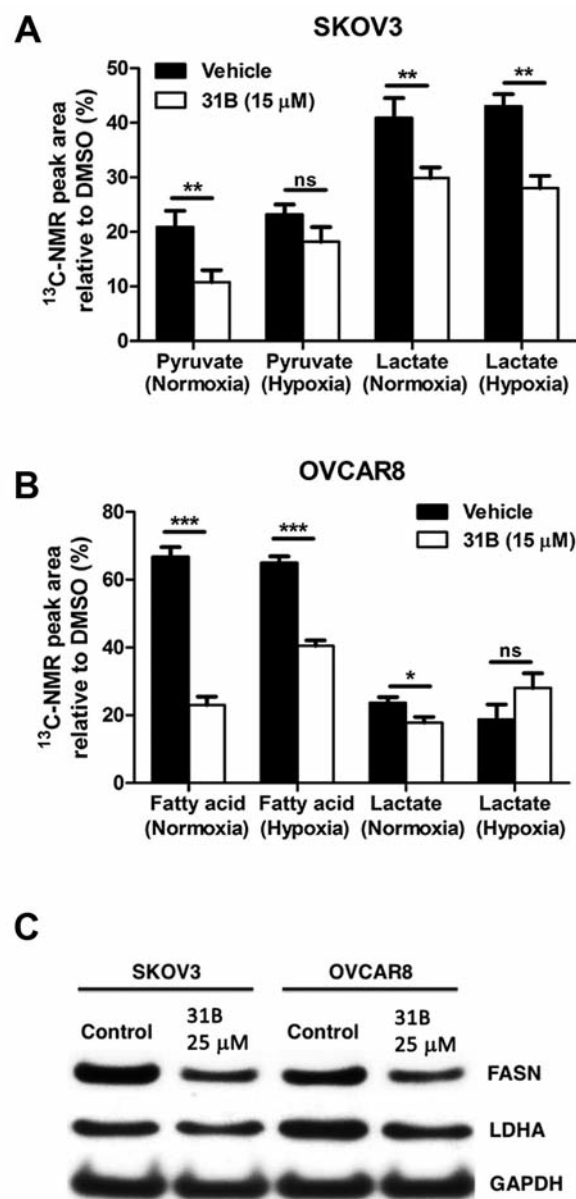With respect to the underlying mode of action of 3-indolylmethanamines, we demonstrated that several

Figure 4. *Modulation of ovarian cancer cell glycolysis and lipogenesis in the presence of 31B. SKOV3 (A) and OVCAR8 (B) cells were grown under normoxia or hypoxia for 18 h in the presence of 31B (15 μM) in medium containing [1,6]^{13}C-glucose. Using ^{13}C-nuclear magnet resonance (NMR), the concentrations of new key metabolites pyruvate, lactate, and fatty acid were quantified. C: SKOV3 and OVCAR8 cells were treated with 25 μM 31B or vehicle for 18 h and lysates were probed by western blot with primary antibodies against fatty acid synthase (FASN), lactate dehydrogenase A (LDHA), and glyceraldehyde 3-phosphate dehydrogenase (GAPDH) Data are the mean±SEM **p<0.001,***p<0.0001.*

apoptotic markers were induced in the presence of 31B, such as executioner caspase-3, causing protein degradation and cell death (13), and the degradation of PARP1 leading to a compromised ability of ovarian cancer cells to repair DNA

damage (14). 31B also activated MAP kinases p38 and SAPN/JNK, which are known to regulate transcription factors such as p53, inducing apoptosis and cell-cycle arrest (15). Besides the induction of multiple apoptotic pathways, reduced tumor formation was partially caused by a compromised *de novo* production of fatty acids due to lower expression of FASN in the tumor.

In vitro experiments using ^{13}C-labeled glucose clearly demonstrated that 31B down-regulated the production of lactate and its glycolytic precursor, pyruvate. In addition, expression levels of FASN and LDHA were shown to be reduced, thus, connecting metabolic impairment to transcriptional inhibition. Jardé *et al.* showed that CCT036477 inhibited major WNT target genes such as achaete-scute complex homolog 2 (*Ascal2*), ephrin type-B receptor 2 (*Ephb2*), leucine-rich repeat-containing G-protein coupled receptor 5 (*Lgr5*) and T-cell lymphoma invasion and metastasis 1 (*Tiam1*) (16). In addition, our group showed that 31B and PS121912 modulate the expression of VDR target genes and oncogenes (6-8).

Thus, the developed 3-indolylmethanamines, despite their reactivity towards nucleophilic residues, exhibit remarkable selectivity among different biomolecules, that enables them to cross cell membranes and interact selectively with transcription factors. In case of the Wnt inhibitor CCT036477, high concentrations can lead to impaired development of *Xenopus laevis* or *Danio rerio* embryos at concentrations of 20-75 μmol/l (5). For 31B and PS12192 at lower concentrations, we observed inhibition of cancer cell growth *in vivo*, without any signs of toxicity. On the molecular level, at pH 7 3-indolylmethanamines may require for a localized acidic center of a protein to enable protonation of the aniline nitrogen. In addition, the proximity of a nucleophilic center for reaction may be necessary to successfully compete with the surrounding weakly nucleophilic water molecules that will convert 3-indolylmethanamines into inactive 3-indolylmethanalcohols (6). Thus, it can be suggested that the selectivity of 3-indolylmethanamines is determined by the molecular residue arrangement of target proteins. These targets, including VDR and members of the WNT pathway, mediate the unique properties of 3-indolylmethanamines such as transcriptional inhibition and anticancer properties. The therapeutic window of these compounds is structurally dependent and has been shown to be non-toxic in rodents up to a dosage of 20 mg/kg (used in pilot study). Two major pathways of anti-proliferation were identified for 31B, which include apoptosis and down-regulation of glycolytic and lipogenic pathways. Future studies will be focused on the identification of other targets modulated by 3-indolylmethanamines, as well as their application in specific *in vivo* ovarian cancer models.

References

1 Erspamer V: Pharmacology of indole-alkylamines. Pharmacol Rev *6*: 425-487, 1954.

2 Snyder HR and Curtis WS: A convenient synthesis of DL-tryptophan. JACS *66*: 350-351, 1943.

3 Gill NS, James KB, Linos F and Potts K: P-Acylethylation with ketonic mannich bases. The synthesis of some diketones, ketonic sulfides, nitroketones and pyridines. JACS *74*: 4923-4928, 1952.

4 Leete E and Marion L: The hydrogenolysis of 3-hydroxymethylindole and other indole derivatives with lithium aluminium hydride. Can J Chem *31*: 775-784, 1953.

5 Ewan K, Pajak B, Stubbs M, Todd H, Barbeau O, Quevedo C, Botfield H, Young R, Ruddle R, Samuel L, Battersby A, Raynaud F, Allen N, Wilson S, Latinkic B, Workman P, McDonald E, Blagg J, Aherne W and Dale T: A useful approach to identify novel small-molecule inhibitors of Wnt-dependent transcription. Cancer Res *70*: 5963-5973, 2010.

6 Nandhikonda P, Lynt WZ, McCallum MM, Ara T, Baranowski AM, Yuan NY, Pearson D, Bikle DD, Guy RK and Arnold LA: Discovery of the first irreversible small molecule inhibitors of the interaction between the vitamin D receptor and coactivators. J Med Chem *55*: 4640-4651, 2012.

7 Sidhu PS, Nassif N, McCallum MM, Teske K, Feleke B, Yuan NY, Nandhikonda P, Cook JM, Singh RK, Bikle DD and Arnold LA: Development of novel Vitamin D receptor-coactivator inhibitors. ACS Med Chem Lett *5*: 199-204, 2014.

8 Sidhu PS, Teske K, Feleke B, Yuan NY, Guthrie ML, Fernstrum GB, Vyas ND, Han LL, Preston J, Bogart JW, Silvaggi NR, Cook JM, Singh RK, Bikle DD and Arnold LA: Anticancer activity of VDR-coregulator inhibitor PS121912. Cancer Chemoth Pharm *74*: 787-798, 2014.

9 Peiffer L, Poll-Wolbeck SJ, Flamme H, Gehrke I, Hallek M and Kreuzer KA: Trichostatin A effectively induces apoptosis in chronic lymphocytic leukemia cells via inhibition of Wnt signaling and histone deacetylation. J Cancer Res Clin Oncol *140*: 1283-1293, 2014.

10 Kaufmann SH, Desnoyers S, Ottaviano Y, Davidson NE and Poirier GG: Specific proteolytic cleavage of poly(ADP-ribose) polymerase: an early marker of chemotherapy-induced apoptosis. Cancer Res *53*: 3976-3985, 1993.

11 Ma Y, Ren Y, Han EQ, Li H, Chen D, Jacobs JJ, Gitelis S, O'Keefe RJ, Konttinen YT, Yin G and Li TF: Inhibition of the Wnt-beta-catenin and Notch signaling pathways sensitizes osteosarcoma cells to chemotherapy. Biochem Biophys Res Commun *431*: 274-279, 2013.

12 Sidhu PS, Teske K, Feleke B, Yuan NY, Guthrie ML, Fernstrum GB, Vyas ND, Han L, Preston J, Bogart JW, Silvaggi NR, Cook JM, Singh RK, Bikle DD and Arnold LA: Anticancer activity of VDR-coregulator inhibitor PS121912. Cancer Chemother Pharmacol *74*: 787-798, 2014.

13 Thornberry NA and Lazebnik Y: Caspases: enemies within. Science 281: 1312-1316, 1998.

14 Rouleau M, Patel A, Hendzel MJ, Kaufmann SH and Poirier GG: PARP inhibition: PARP1 and beyond. Nat Rev Cancer *10*: 293-301, 2010.

15 Vogelstein B, Lane D and Levine AJ: Surfing the p53 network. Nature *408*: 307-310, 2000.

16 Jarde T, Evans RJ, McQuillan KL, Parry L, Feng GJ, Alvares B, Clarke AR and Dale TC: *In vivo* and *in vitro* models for the therapeutic targeting of Wnt signaling using a Tet-ODeltaN89beta-catenin system. Oncogene *32*: 883-893, 2013.